



A comparative study of nitrate removal from aqueous solutions using zeolite, nZVI–zeolite, nZVI and iron powder adsorbents

Masoud Moradi^a, Omol Banin Naej^b, Ali Azari^{a,c}, Anoushiravan Mohseni Bandpei^d, Ahmad Jonidi Jafari^b, Ali Esrafil^b, Roshanak Rezaei Kalantary^{b,e,*}

^aResearch Center for Environmental Determinants of Health, Kermanshah University of Medical Sciences, Kermanshah, Iran, email: mahfooz60@gmail.com

^bDepartment of Environmental Health Engineering, School of Public Health, Iran University of Medical Sciences, Tehran, Iran, emails: omolbaninnaej@gmail.com (O.B. Naej), ahmad_jonidi@yahoo.com (A.J. Jafari), A_esrafil@yahoo.com (A. Esrafil)

^cDepartment of Environmental Health Engineering, School of Public Health, Tehran University of Medical Sciences, Tehran, Iran, email: aliali2890@yahoo.com

^dDepartment of Environmental Health Engineering, School of Public Health, Shahid Beheshti University of Medical Sciences, Tehran, Iran, email: a.mohseni8@yahoo.com

^eResearch Center for Environmental Health Technology (RCEHT), Iran University of Medical Sciences, Tehran, Iran, Tel. +98 9123234586; email: rezaei.k.r2016@gmail.com

Received 4 October 2016; Accepted 14 February 2017

ABSTRACT

Nitrate is one of the most important pollutants causing some problems in the environment, particularly in water bodies. In this study, batch adsorption experiments were performed to investigate the feasibility of the adsorbents: zeolite, nano zero-valent iron (nZVI)–zeolite, nZVI and iron powder for nitrate removal from aqueous solutions. Also, the effects of different operating parameters like pH, temperature, contact time, adsorbent dosage and initial nitrate concentration were investigated. Results indicated that nitrate removal was strongly pH dependent. The maximum removal (96.5%) occurred at pH = 3 for nZVI–zeolite. Experimental equilibrium data were fitted to the pseudo-second-order and Langmuir isotherm models and the adsorption capacities of zeolite, nZVI–zeolite, nZVI and iron powder for nitrate were 12.804, 18.939, 17.064 and 9.671 mg/g, respectively. Total nitrogen loss was obtained at 13, 10 and 8% for nZVI–zeolite, nZVI and iron powder, respectively. The reduction of nitrate to ammonium, and nitrate adsorption by the adsorbents were main mechanisms in nitrate removal. Thermodynamic studies indicated that the adsorption process was spontaneous and exothermic and the adsorption capacity slightly dropped with increasing temperature. It can be concluded that the adsorbents, especially nZVI–zeolite, could decrease nitrate to meet standard limits.

Keywords: Nitrate removal; Zeolite; nZVI–zeolite; nZVI; Iron powder

1. Introduction

Nitrate is a wide spread pollutant of surface water and groundwater and has become an increasingly important problem for many locations around the world. High nitrate levels in surface water can cause serious threats in aqueous

phase such as increase of alga growth, which usually leads to eutrophication [1]. Septic system leakage, discharge of untreated sanitary and industrial wastes in unsafe manner, agriculture fertilizer and landfill leachate are the major potential sources of nitrate [2]. High levels of nitrate in drinking water have been associated with serious health issues like methemoglobinemia (blue baby syndrome in babies) miscarriages and non-Hodgkin's lymphoma leading to the formation of nitrosamine which is related to cancer [2,3].

* Corresponding author.

The regulatory health limits of nitrate recommended by the US Environmental Protection Agency (EPA) and European Union are 10 and 25 mg/L, respectively [2]. In order to treat nitrate-laden wastewaters, various methods including biological (autotrophic and heterotrophic denitrification), chemical (chemical reduction, adsorption and ion exchange) and physical (electrodialysis or reverse osmosis) processes have been applied [4,5]. Although these methods are nearly efficient, there are some serious disadvantages like generation of by-products and high costs of operation. Addition of a carbon source and biomass waste is a principal drawback of biological processes. And, high operational costs and inactivation of electrode are the main limitations of reverse osmosis and ion exchange and electrodialysis, respectively. Waste brine disposal and renewal of costly ion-exchange resin are the restrictions of utilizing this method [6]. However, adsorption seems to be enough attractive because of its cheapness, effectiveness and ease of design and operation; different adsorbents, like active coal, clays, functionalized mesoporous materials and surfactant-modified zeolites, have been employed for nitrate removal from aqueous solutions. Zeolite has broadly been used for removal of water pollutants, due to the large specific surface area, cation exchange capacity, low cost and mechanical strength; moreover, zeolite particles have a net negative surface charge in water that affords hydrophilic nature making them inappropriate for the removal of anionic and hydrophilic pollutants [7]. Besides, in recent years, great attention has been taken to water treatment by means of nanomaterials due to benefits like large surface area and enhanced [8]. Zero-valent iron, which is one of the best nanomaterials, has widely been studied for removal of water contaminants such as chlorinated solvents and nitro aromatics in aqueous phase; it has been illustrated that Fe^0 has proper potential to reduce nitrate (NO_3^-) in water; also, water treatment by using zero-valent iron is relatively cheap and easy [3]. Fe^0 is reduced to ferrous or ferric ions by direct exchange of electron with nitrate or hydrogen gas generated.



These iron by-products can affect the sustainability of Fe^0 in treatment system [9]. ZVI particles show strong affinity to agglomerate into larger particles due to the high surface energy and intrinsic magnetic interaction. All these reasons can result in a decrease in both effective surface area and removal efficiency. In addition, the separation and recycling of bare ZVI particles are extremely difficult [10]. The use of solid carriers is a proper way to solve these challenges; zeolites, having a three-dimensional structure, uniform pores and channel systems, can be an appropriate alternative for the exchange of cations [11].

Chen and Li [12] claimed that nitrate can be reduced to ammonium via nanoscale zero-valent iron particles and zeolite. Since ammonium is still a dangerous pollutant, it is not entered into the environment by adsorption, which is done by zeolite. The findings of another study by Fatemina and Falamaki [13], who investigated nitrate removal by means of zero-valent nano sized iron/

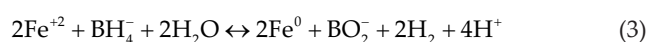
clinoptilolite modified with zero-valent copper, illustrated that the nitrate reduction improved when small contents of Cu^0 were added to the freshly prepared Fe^0 /zeolite composite. Sepehri et al. [14], concluded that zeolite supported with nano zero-valent iron (nZVI) materials both prevented the agglomeration of nZVI into larger particles and had high flexibility and activity for the removal of nitrate. Thus, an improvement in removal efficiency of nitrate can be expected when Fe^0 is combined with zeolite. The aim of the current study was to evaluate nitrate removal from aqueous solutions by using zeolite, nZVI-zeolite, nZVI and iron powder.

2. Methods

The zeolite samples were sieved and the fractions with the size of 1–2 mm were collected for use. The commercial iron powder with the particle size of 10–45 μm and chemicals: ferrous sulfate heptahydrate ($\text{FeSO}_4 \cdot 7\text{H}_2\text{O}$), sodium borohydride (NaBH_4), sodium hydroxide (NaOH), hydrochloric acid (HCl) and acetone were of analytical grade and purchased from Merck Co., Germany.

2.1. Zeolite supported by nano zero-valent iron (nZVI-zeolite)

The zeolite particles were washed with ultrapure water and dried in an oven at 105°C for 24 h. Next, the particles were immersed in hydrochloric acid (20%) for 24 h to remove surface impurities and then washed extensively with distilled water [7]. Afterward, 1 g of zeolite was transferred to N_2 -purged ferrous sulfate solution for 3 h. The obtained slurry was diluted five times using a mixture of ethanol and deionized water (1:1), 100 mL of NaBH_4 (0.2 M) was then added dropwise into the slurry at 25°C with magnetic stirring and N_2 bubbling for 30 min. Ferrous iron (Fe^{2+}) was reduced according to the following reaction:



Then, zeolite-supported nZVI was separated from the mixture and washed with acetone for three times; it was vacuum dried at 60°C and stored in an N_2 -purged desiccator [15].

2.2. Batch experiments

One hundred milliliter of the nitrate solution was transferred into 250 mL conical flasks for the batch experiments by shaking at 200 rpm and 4 h of contact time under N_2 -purged conditions.

2.3. Adsorption studies

The experiments were performed at the initial nitrate concentration of 100 mg/L and adsorbent dosage of 7.5 g/L. The effect of adsorbent dosage was studied via addition of 1–10 g/L of the adsorbents including zeolite, zeolite supported by nZVI and iron powder. The initial pH of the nitrate solution was adjusted in the range from 2 to 9 by using 0.1 M HCl or 0.1 M NaOH solutions.

2.4. Kinetic and isotherm study

Kinetic studies were carried out at different nitrate concentrations (10–500 mg/L) at certain intervals (5–360 min). And, isotherm studies were conducted at different initial nitrate concentrations (10–500 mg/L). Adsorption capacities of the adsorbents were calculated at equilibrium using the following equation [16]:

$$q_e = \frac{(C_0 - C_e)V}{M} \quad (4)$$

where q_e (mg/g) is adsorption capacity, C_0 (mg/L) is initial nitrate concentration, C_e (mg/L) is the final or the equilibrium concentration of nitrate, V is the experimental solution volume (L) and M is the weight of the adsorbents (g).

2.5. Analysis

The concentrations of nitrate were determined by the standard colorimetric method using a UV/VIS spectrophotometer (7400CE CECIL). Thus, nitrate concentration was measured and calculated by UV absorbance at 220 nm and corrected by subtracting a second absorbance at 275 nm, according to the standard method (NO_3^- -4500). Moreover, nitrite and total nitrogen contents were detected based on the standard methods (NO_2^- -4500) and (N-4500), respectively [17]. The surface morphology and particle size were investigated by a scanning electron microscope (SEM; Philips XL30). The crystal structure of the adsorbents was carried out by quantitative X-ray diffraction (XRD; Quantachrome, NOVA 2000, USA). The fourier transform infrared radiation (FTIR) spectrum of each sample was performed using a FTIR spectrophotometer (WQF-510 Model), in the range of 400–4,000 cm^{-1} . And, the transmission electron microscopy (TEM) technique (PHILIPS, The Netherlands) was used for determination of the size and form of the adsorbents.

3. Results and discussion

3.1. Physical characterization

Fig. 1 shows the surface morphology (SEM) of the adsorbents. These images confirmed that nano scale zero-valent iron did not cover uniformly on the zeolite's surface and was patchy in some sections of the surface. Fig. 2 presents the energy dispersive X-Ray (EDX) analysis; this method was applied to ensure the presence of elements in the structure of the synthesized adsorbent. As shown in Fig. 3, there are some peaks for iron proving the existence of Fe on the surface of the adsorbent. The analysis also revealed the presence of Si, Al and Ca corresponding to the zeolite structure. Thus, these results suggest that Fe occupied the majority of the adsorbent surface. Fig. 3 depicts the XRD patterns of bare zeolite, nZVI and nZVI–zeolite in the range of $2\theta = 5\text{--}685$ (i.e., $\text{Cu K}\alpha$ radiation). The XRD pattern illustrated that zeolite was mainly comprised of heulandite ($2\theta = 10.0^\circ$, 19.0° , 22.7° and 30.0°) and small amount of quartz ($2\theta = 21.0^\circ$, 27.0° and 36.5°) [18]. A cubic spinel structure of the magnetite is shown via the peaks at $2\theta = 44.9^\circ$ and 65.1° for the nZVI particles that are marked by their indices (110) and (200), respectively. The peaks accord closely those gained from the JCPDS card no. 65-4899 for magnetite; that is, these peaks can be indicative

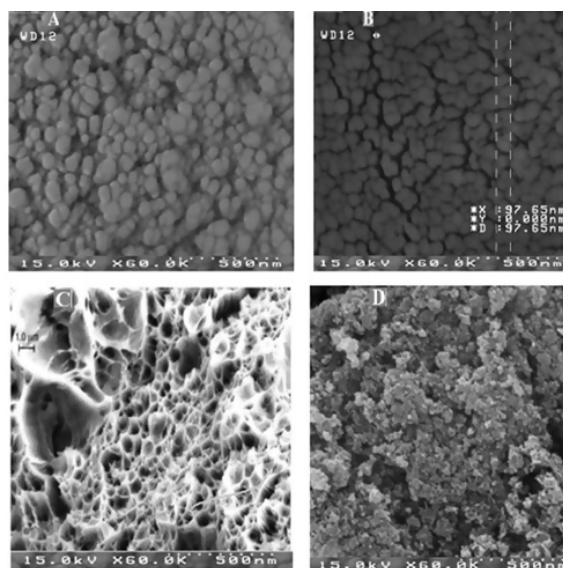


Fig. 1. SEM microimages of the zeolite (A), nZVI–zeolite particles (B), iron powder (C) and nZVI (D).

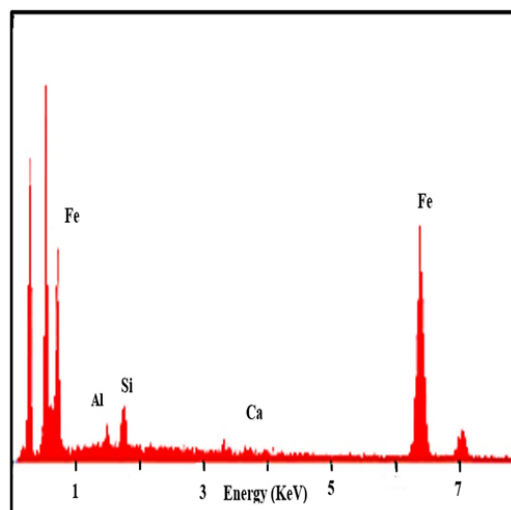
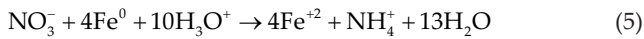


Fig. 2. EDX patterns of zeolite supported zero-valent iron particles (nZVI–zeolite).

of generation of magnetite nZVI [10]. It should be noted that the cubic phase of nZVI was remained unchanged after the mesoporous zeolite-loading phase, which can be because of the peaks seen in the pattern of synthesized nZVI–zeolite [19]. But a decrease in the intensity of Fe^0 peaks was observed in nZVI–zeolite structure and a new peak (37.5°) indicating Fe_3O_4 was seen; this illustrated that nZVI oxidized in ambient conditions over the synthesis and preservation. Moreover, a detectable damage to the zeolite framework was not seen [20]. As a whole it can be concluded that nZVI–zeolite was effectively synthesized and the resulting composite could be separated from the aqueous phase through a magnet. Fig. 4 shows the FTIR spectra for nZVI–zeolite. Zeolites were obtained in the range of 400–4,000 cm^{-1} . Two strong bands at 1,040 and 1,134 cm^{-1} correspond to the external vibrations between the (Al and Si) O_4 tetrahedrons. The IR band at 624 cm^{-1} is related

direct participation in the redox reaction and (b) adsorption of nitrate [12]. But at $\text{pH} > 4$, nitrate reduction was insignificant, because a passive oxide layer (ferrous hydroxide) is formed causing a significant decrease in iron corrosion [24]; consequently, higher nitrate removal happened in acidic conditions. Yang and Lee [24] revealed that enhanced iron corrosion in acid solution causes rapid reduction of nitrate by Fe^0 at $\text{pH} \leq 4$ as follows:



Fe^0 corrosion is the main electron donor for nitrate reduction producing Fe^{2+} and hydrogen. In pH-buffered solutions, Fe^0 corrosion is necessary for nitrate reduction, which is done by species like $\text{Fe}(\text{OH})_2$ and Fe^{2+} .

Given that $\text{Fe}(\text{OH})_2$ is unstable in anoxic solution ($\text{pH} = 2\text{--}4$), where fast nitrate reduction was expected to be observed. Therefore, the rapid reduction of nitrate can take place at low pH on account of its reaction with hydrogen or Fe^0 [3].

The pH impact on the kinetics of nitrate reduction in acidic conditions can be illuminated in two ways: (a) H^+ ions directly participate in the redox reaction of nitrate reduction following first-order kinetics and (b) H^+ ions affect nitrate adsorption onto reactive sites. Black hydroxide on the surface of the iron grains in the presence of nitrate can be formed due to the release of Fe^{2+} by iron acidic corrosion. The black oxide is unstable and changed over time into other oxides under certain conditions. The black film increases nitrate reduction and causes more iron acidic corrosion than the decrease of the reactivity of Fe^0 [25].

When zeolite and nZVI were used together, the nitrate removal increased due to the synergistic impact of the combined system on the adsorption. Moreover, zeolite provides more adsorptive surface sites for scavenging the reduction products of nitrate and significantly improves the reduction efficiency of nitrate by nZVI [26].

3.3. Effect of adsorbent dosage

Adsorbent dosage is a main factor affecting adsorption capacity and removal efficiency [27]. Fig. 7 presents the effect of different adsorbent dosages on nitrate removal. As can be seen, the removal efficiencies increased from 41.2% to 81.5%, 65% to 99.1%, 59.3% to 96.2% and 57.1% to 89.5% for zeolite, nZVI–zeolite, nZVI and powder iron, respectively. This increase can be attributed to the availability of more active sites and larger surface areas at higher dosages [28]. It was also found that the removal efficiency went up to the optimum value of dosage and beyond which the efficiency leveled off [29], which was because of the overlapping of active sites at higher dosages. Therefore, due to the conglomeration of exchanger particles, there was not a considerable increase in the active surface areas [30].

3.4. Fate of nitrate during reduction by nZVI and nZVI–zeolite

Many studies have demonstrated that Fe^0 causes nitrate reduction and produces some nitrogen products [24]. Fig. 8

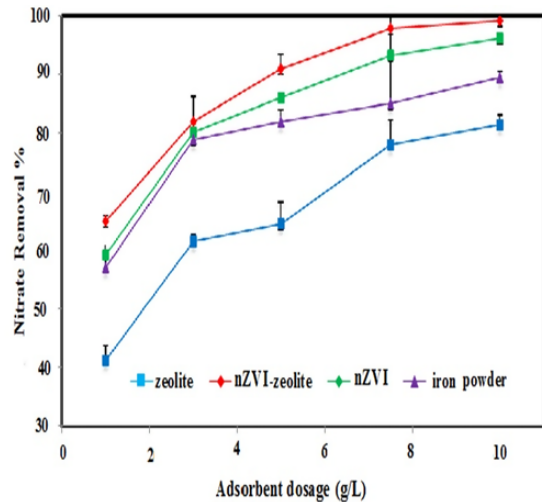
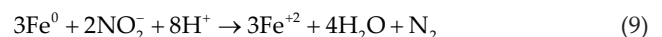
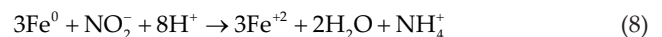
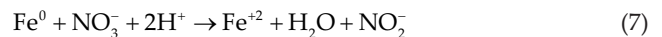


Fig. 7. Effect of adsorbent dosage on the removal of nitrate by different adsorbents (initial concentration of nitrate 100 mg/L, optimum pH and contact time for each adsorbent).

shows the nitrogen species concentration changes for nZVI–zeolite and nZVI. As illustrated, at first, there was some nitrate in the solution and the end products were largely composed of nitrite, ammonium and nitrogen gas [31]. The results showed that reduction of nitrate to ammonium and then ammonium adsorption was the main phenomena for nitrate removal; thus, the amount of nitrate reduction to ammonium was 81%, 78% and 76% for nZVI–zeolite, nZVI and iron powder, respectively. In final solution, the sum of nitrate, nitrite and ammonium is always less than the influent total nitrogen [9].

The loss of total nitrogen (TN) concentration after 24 h was explained to be due to the nitrogen gas [6]. In this study, the findings showed the TN losses were 13%, 10% and 8% for nZVI–zeolite, nZVI and iron powder, respectively. This can be due to more adsorption of nitrogen compound by nZVI–zeolite $>$ nZVI $>$ iron powder [31]. In addition, nitrite was generated in the first stage and the peak concentration was obtained at 10 min, and then transformed into ammonium after 70 min as follows:



3.5. Effect of initial concentration and adsorption isotherm

The percentage removal of nitrate vs. initial nitrate concentration has been shown in Fig. 9. The removal efficiency of nitrate decreased with raising its initial content [30]. With increasing initial concentration of nitrate from 10 to 500 mg/L, the nitrate removal efficiency decreased from 99.9% to 26.9%, 99.9% to 30.9%, 99.9% to 29.1% and 99.9% to 28% for zeolite, nZVI–zeolite, nZVI and powder iron, respectively. This decrease can be attributed to this fact that concentration gradient acts as a driving force and overcomes mass transfer

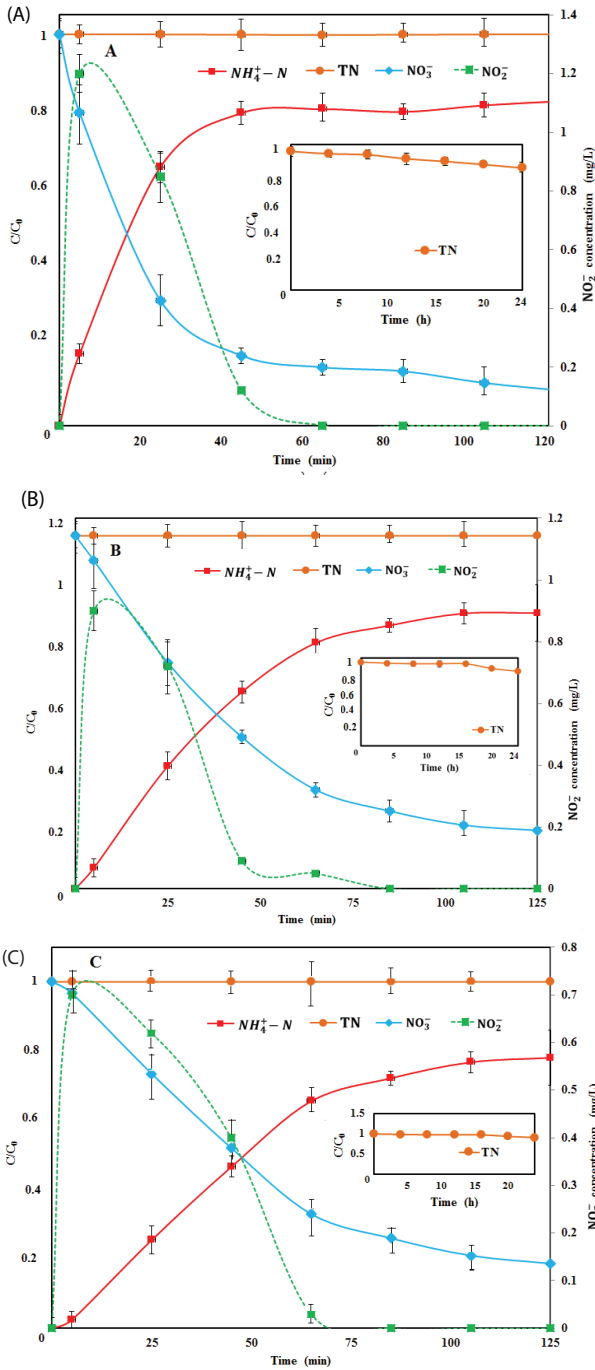


Fig. 8. (A) The concentration change of nitrogen species during the nitrate reduction by nZVI-zeolite. (B) The concentration change of nitrogen species during the nitrate reduction by nZVI. (C) The concentration change of nitrogen species during the nitrate reduction by iron powder.

resistance between bulk solution and adsorbent surface [32]. The adsorption isotherms were modeled using the Langmuir and Freundlich models and the results are as follows:

Langmuir model:

$$q_e = \frac{Q_m b C_e}{1 + b C_e} \quad (10)$$

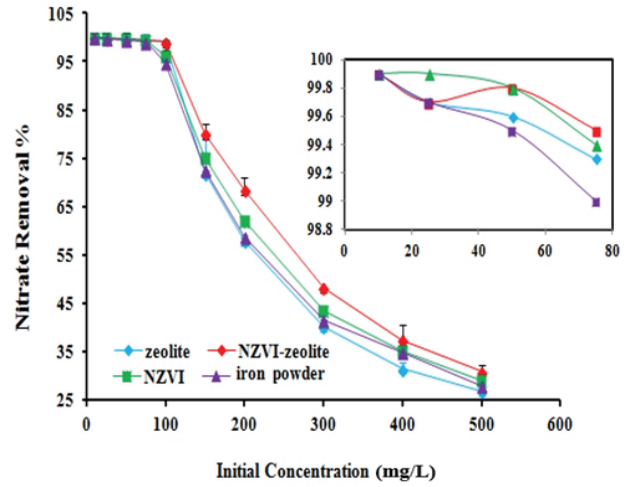


Fig. 9. Percentage removal of nitrate by different adsorbents vs. initial nitrate concentration (optimum adsorbent dosage, pH and contact time for each adsorbent).

where q_e is the amount of adsorbed material at equilibrium (mg/g), C_e is the equilibrium concentration (mg/L), b is the affinity parameter or Langmuir constant (L/mg) and Q_m is the maximum adsorption capacity (mg/g).

Freundlich model:

$$q_e = K_f C_e^{1/n} \quad (11)$$

where K_f and n are the Freundlich constants related to the adsorption capacity and intensity, respectively [33]. Moreover, the important aspect of the Langmuir isotherm can be explained in terms of a dimensionless constant under the name of separation factor (R_L) (Eq. (12)):

$$R_L = \frac{1}{(1 + b C_0)} \quad (12)$$

where C_0 is the initial nitrate concentration in the liquid phase (mg/L).

3.6. Initial concentration of nitrate

The form of the isotherm is presented by the value of R_L as follows: unfavorable ($R_L > 1$), linear ($R_L = 1$), favorable ($0 < R_L < 1$) or irreversible ($R_L = 0$); and the R_L values between 0 and 1 show favorable adsorption. In the present study, the R_L value was found to be between 0 and 1 proving that the adsorption is a favorable process for all adsorbents [34]. The detailed information of the Langmuir and Freundlich constants and the calculated coefficients has been shown in Table 1 and Figs. S2 and S3. It was found that the correlation coefficient (R^2) obtained indicated that the Langmuir isotherm had the best fit with the experimental data (>0.99). This implies that the process of nitrate adsorption onto the adsorbents follows a monolayer and regular and porous structure [35]. The adsorption happened at the functional groups/binding sites on the surface of the adsorbents confirming that it is a monolayer adsorption [6]. Since the adsorption capacities of zeolite, nZVI-zeolite, nZVI and powder iron were, respectively,

12.804, 18.939, 17.064 and 9.671 mg/g; these are indicative of the large surface area of the nZVI–zeolite adsorbent. The maximum values of K_f for the nZVI–zeolite and other adsorbents show that the amount of adsorption is higher than that of other adsorbents. In this study, n values were found to be between 3.5 and 5.5. Mathematical calculation of n presents that the adsorption process is desirable when it is between 1 and 10 and the lower n , the higher adsorption intensity will be obtained [29].

3.7. Effect of time and adsorption kinetics

The effect of contact time on nitrate adsorption onto the adsorbents has been shown in Fig. S4. The adsorption efficiency increased dramatically up to 30 min and then gradually reached the equilibrium state at 60 min; apparently, the amount of the adsorption increased dramatically with raising time.

It should be noted that the removal efficiencies were reached 51.2%, 91.6%, 87.2% and 83.1% for zeolite, nZVI–zeolite, nZVI and powder iron, respectively, only in 30 min. The vacant active sites on the surface of the adsorbents are occupied by the adsorbate over time, which, in turn, leads to the saturation of adsorbent surfaces [28]. Adsorption kinetics is an important characteristic for evaluating the efficiency of adsorption. In order to examine controlling mechanisms of the adsorption process such as mass transfer and chemical reaction, several kinetic models are used to test the experimental data like the pseudo-first-order (Eq. (13)), pseudo-second-order (Eq. (14)), intraparticle diffusion (Eq. (15)) models [36].

Pseudo-first order:

$$\log\left(1 - \frac{q_t}{q_e}\right) = \frac{-K_1}{2.302} t \tag{13}$$

Table 1 Isotherm constant for different adsorbents

Adsorbent	Langmuir				Freundlich		
	q_{max}	b	R_L	R^2	K_f	n	R^2
Zeolite	12.8	0.57	0.15	0.9944	3.28	3.5	0.7284
nZVI–zeolite	18.93	0.3	0.25	0.9922	7.83	5.5	0.9142
nZVI	17	0.152	0.152	0.9917	5.67	4.82	0.9667
Powder iron	9.67	0.71	0.12	0.9929	2.88	3.84	0.56

Table 2 Kinetic constant for different adsorbents

Adsorbent	q_e (experimental)	First-order kinetic model			Second-order kinetic model			Intraparticle diffusion model	
		K_1	q_e	R^2	K_2	q_e	R^2	K_i	R^2
nZVI–zeolite	13.06	0.0011	3.84	0.082	0.08	13.15	0.9996	0.07	0.215
nZVI	12.82	0.0013	3.24	0.095	0.052	13.02	0.9989	0.1129	0.258
Zeolite	12.67	0.0017	2.68	0.1812	0.0256	12.97	0.9983	0.1631	0.33
Iron powder	12.13	0.0019	2.14	0.2539	0.0122	12.65	0.9955	0.2555	0.38

Pseudo-second order:

$$\frac{t}{q_t} = \frac{t}{q_e} + \frac{1}{K_2 q_e^2} \tag{14}$$

Intraparticle diffusion:

$$q_t = K_i t^{0.5} + I \tag{15}$$

where q_e (mg/g) and q_t (mg/g) are the amounts of nitrate adsorbed by the adsorbents at the equilibrium and at different time intervals, respectively, K_1 (1/min) and K_2 (g/mg min) are the pseudo-first-order and pseudo-second-order rate constants, respectively, and K_i is the intraparticle diffusion rate constant (mg/g min^{0.5}). The validity of the models can be checked by the linear plots [$\log\left(1 - \frac{q_t}{q_e}\right)$ vs. t], [t/q_t vs. t] and [q_t vs. $t^{0.5}$]. The kinetic parameters were calculated from Eqs. (13)–(15). Table 2 and Figs. S5–S7 present the adsorption capacities of different concentrations of nitrate on the adsorbents.

3.8. Adsorption thermodynamics

Thermodynamics studies are very important in adsorption processes because they contribute to understand that the particular adsorption process is physical or chemical, spontaneous or non-spontaneous and also exothermic or endothermic [37]. In this research, the interrelationship between temperature, entropy and enthalpy variables was investigated (Table 3). The van't Hoff equation was utilized to assess the impact of temperature on the adsorption process:

$$\ln K_c = \frac{\Delta S^0}{R} - \frac{\Delta H^0}{RT} \tag{16}$$

The constant K_c is expressed as follows:

$$K_c = \frac{q_e}{C_e} \tag{17}$$

where R is gas constant (8.314 J/mol/K), T is temperature (K) and K_c is the equilibrium constant ($K_c = q_e/C_e$). In $K_c = q_e/C_e$, q_e is the adsorption capacity at equilibrium (mol/g or mg/g) and C_e is the adsorbate concentration at equilibrium (mg/L or mol/L). The values of enthalpy change (ΔH^0 , kJ/mol) and entropy change (ΔS^0 , kJ/mol K) can be calculated from the slope and intercept of the linear plot between $\ln K_c$ and $1/T$.

Table 3
Adsorption thermodynamic parameters for nitrate adsorption on the different adsorbents

	Temperature (K)	q_e (mg/g)	ΔG° (kJ/mol)	ΔH° (kJ/mol)	ΔS° (J/mol/K)
Zeolite	293	9.29	-4.36	-6.54	-0.05
	303	9.17	-4.78		
	323	9.11	-3.08		
nZVI-zeolite	293	9.7	-2.86	-14.56	-0.04
	303	9.62	-2.38		
	323	9.48	-1.66		
nZVI	293	9.51	-1.62	-12.21	-0.036
	303	9.42	-1.24		
	323	9.24	-0.52		
Iron powder	293	9.37	-0.97	-9.12	-0.03
	303	9.28	-0.63		
	323	9.13	-0.13		

The standard free energy (ΔG° , kJ/mol) is linked to the changes of ΔH° , ΔS° and temperature (T) based on Eq. (18).

$$\Delta G^\circ = \Delta H^\circ - (T\Delta S^\circ) \text{ or } \Delta G = -RT \ln K_c \quad (18)$$

The feasibility of the process and the spontaneous nature of adsorption are confirmed by the negative values of ΔG° . At high temperatures, the adsorption process gets more desirable because of a decrease in the negative value of ΔG° . The non-spontaneous nature of the adsorption process is illustrated by positive ΔG° values [32]. An energy barrier is also defined by the positive value of ΔG° . When the ions are entered from the solution into the particle surface, some of water molecules forming the hydration shell of the ions are stripped off and also the degrees of freedom of ions declines. The adsorption has a physisorption mechanism at $0 < \Delta G^\circ > -20$, physisorption with chemisorption at $-20 < \Delta G^\circ > -80$ and only chemisorption at $-80 < \Delta G^\circ > -400$ [38].

The exothermic adsorption process is expected when there are a negative value of ΔH° and a reversed trend between $\ln(K_c)$ and temperature. That is, at higher temperatures, the sorbent has low affinity toward the adsorbate. The enhanced randomness at the solid/solution interface over the adsorption is predicted to happen when the ΔS° value is positive; additionally, it illustrates an increase in the degrees of freedom adsorbed species [39].

4. Conclusion

Zeolite has good adsorption properties due to its channel structure, large specific surface, sorption capacities, low cost and mechanical strength. The maximum percentage removal of nitrate occurred at the pH values of 5 and 3 for zeolite and other adsorbents, respectively. This study showed that the adsorptive effectiveness of nitrate removal by nZVI-zeolite was higher than that of other adsorbents for high sorption capacities and enhancing the removal efficiency by Fe^0 .

XRD, SEM, TEM and EDX analyses revealed that nZVI-zeolite had been synthesized properly. Results showed that

the nitrate adsorption on the adsorbents was strongly pH dependent. Electrostatic repulsion of anionic nitrate by the negatively charged surface of the adsorbents, at higher pHs, caused a sharp decrease in nitrate adsorption. The removal efficiency of nitrate increased by increasing adsorbent dosage, resulting in availability of more active sites and larger surface area. In addition, experimental equilibrium data were best fitted to the pseudo-second-order and Langmuir isotherm models and the adsorption capacities of nitrate were 12.804, 18.939, 17.064 and 9.671 mg/g for zeolite, nZVI-zeolite, nZVI and iron powder, respectively. TN loss was obtained at 13%, 10% and 8% for nZVI-zeolite, nZVI and iron powder, respectively. The reduction of nitrate to ammonium, and its adoption by the adsorbents were the main mechanisms for nitrate removal. Thermodynamic studies indicated that the adsorption process was spontaneous, exothermic and the adsorption capacity slightly dropped with increasing temperature. It can be concluded that the adsorbents, especially nZVI-zeolite, and reduction can decrease nitrate to meet standard limits.

Acknowledgment

The authors wish to acknowledge the invaluable cooperation and support from the deputy and chemistry laboratory staff of Iran University of Medical Sciences for facilitating the issue of this study.

References

- [1] J. Rodríguez-Maroto, F. García-Herruzo, A. García-Rubio, C. Gómez-Lahoz, C. Vereda-Alonso, Kinetics of the chemical reduction of nitrate by zero-valent iron, *Chemosphere*, 74 (2009) 804–809.
- [2] D.-W. Cho, C.-M. Chon, B.-H. Jeon, Y. Kim, M.A. Khan, H. Song, The role of clay minerals in the reduction of nitrate in groundwater by zero-valent iron, *Chemosphere*, 81 (2010) 611–616.
- [3] J. Li, Y. Li, Q. Meng, Removal of nitrate by zero-valent iron and pillared bentonite, *J. Hazard. Mater.*, 174 (2010) 188–193.
- [4] J. Schick, P. Caullet, J.-L. Paillaud, J. Patarin, C. Mangold-Callarec, Batch-wise nitrate removal from water on a surfactant-modified zeolite, *Microporous Mesoporous Mater.*, 132 (2010) 395–400.

- [5] M. Pirsahab, M. Moradi, H.R. Ghaffari, K. Sharafi, Application of response surface methodology for efficiency analysis of strong non-selective ion exchange resin column (A 400 e) in nitrate removal from groundwater, *Int. J. Pharm. Technol.* 8 (2016) 11023–11034.
- [6] Y.-H. Hwang, D.-G. Kim, H.-S. Shin, Mechanism study of nitrate reduction by nano zero valent iron, *J. Hazard. Mater.*, 185 (2011) 1513–1521.
- [7] H. Guan, E. Bestland, C. Zhu, H. Zhu, D. Albertsdottir, J. Hutson, C.T. Simmons, M. Ginic-Markovic, X. Tao, A.V. Ellis, Variation in performance of surfactant loading and resulting nitrate removal among four selected natural zeolites, *J. Hazard. Mater.*, 183 (2010) 616–621.
- [8] M.H. Rasoulifard, S. Khanmohammadi, A. Heidari, Adsorption of cefixime from aqueous solutions using modified hardened paste of Portland cement by perlite; optimization by Taguchi method, *Water. Sci. Technol.*, 74 (2016) 1069–1078.
- [9] P. Westerhoff, J. James, Nitrate removal in zero-valent iron packed columns, *Water. Res.*, 37 (2003) 1818–1830.
- [10] Y. Zhang, Y. Li, J. Li, L. Hu, X. Zheng, Enhanced removal of nitrate by a novel composite: nanoscale zero valent iron supported on pillared clay, *Chem. Eng. J.*, 171 (2011) 526–531.
- [11] S. Comba, M. Martin, D. Marchisio, R. Sethi, E. Barberis, Reduction of nitrate and ammonium adsorption using microscale iron particles and zeolite, *Water Air Soil Pollut.*, 223 (2012) 1079–1089.
- [12] X. Chen, T. Li, Reduction of Nitrate in Water by Nanoscale Zero-Valent Iron Particles and Zeolite, *IEEE Third International Conference on Bioinformatics and Biomedical Engineering (ICBBE)*, 2009.
- [13] F.S. Fatemina, C. Falamaki, Zero valent nano-sized iron/clinoptilolite modified with zero valent copper for reductive nitrate removal, *Process Saf. Environ. Prot.*, 91 (2013) 304–310.
- [14] S. Sepehri, M. Heidarpour, J. Abedi-Koupai, Nitrate removal from aqueous solution using natural zeolite-supported zero-valent iron nanoparticles, *Soil Water Res.*, 1 (2014) 224–232.
- [15] H. Zhu, Y. Jia, X. Wu, H. Wang, Removal of arsenic from water by supported nano zero-valent iron on activated carbon, *J. Hazard. Mater.*, 172 (2009) 1591–1596.
- [16] K. Sharafi, K. Kavehmi, A. Hossein, R. Roshanak, H. Zargam, S. Hooshmand, M. Masoud, Application of response surface methodology (RSM) for statistical analysis, modeling and optimization of removal of phenol from aqueous solutions by aluminum-modified scoria powder, *Int. Res. J. Appl. Basic Sci.*, 9 (2015) 1789–1798.
- [17] APHA, AWWA, WPCF, Standard Method for the Examination of Water and Wastewater, 21st ed., American Public Health Association, Washington, D.C., USA, 2005, pp. 5–19.
- [18] M. Liu, D. An, L.-a. Hou, S. Yu, Y. Zhu, Zero valent iron particles impregnated zeolite X composites for adsorption of tetracycline in aquatic environment, *RSC Adv.*, 5 (2015) 103480–103487.
- [19] Y.H. Huang, T.C. Zhang, Effects of low pH on nitrate reduction by iron powder, *Water Res.*, 38 (2004) 2631–2642.
- [20] Z. Jiang, L. Lv, W. Zhang, Q. Du, B. Pan, L. Yang, Q. Zhang, Nitrate reduction using nanosized zero-valent iron supported by polystyrene resins: role of surface functional groups, *Water Res.*, 45 (2011) 2191–2198.
- [21] M. Moradi, A. Dehpahlavan, R. Rezaei Kalantary, A. Ameri, M. Farzadkia, H. Izanloo, Application of modified bentonite using sulfuric acid for the removal of hexavalent chromium from aqueous solutions, *Environ. Health Eng. Manage. J.*, 2 (2015) 99–106.
- [22] Z.-x. Chen, X.-y. Jin, Z. Chen, M. Megharaj, R. Naidu, Removal of methyl orange from aqueous solution using bentonite-supported nanoscale zero-valent iron, *J. Colloid Interface Sci.*, 363 (2011) 601–607.
- [23] P. Ganesan, R. Kamaraj, S. Vasudevan, Application of isotherm, kinetic and thermodynamic models for the adsorption of nitrate ions on graphene from aqueous solution, *J. Taiwan Inst. Chem. Eng.*, 44 (2013) 808–814.
- [24] G.C. Yang, H.-L. Lee, Chemical reduction of nitrate by nanosized iron: kinetics and pathways, *Water Res.*, 39 (2005) 884–894.
- [25] Y.H. Huang, T.C. Zhang, Effects of low pH on nitrate reduction by iron powder, *Water Res.*, 38 (2004) 2631–2642.
- [26] Y.J. Oh, H. Song, W.S. Shin, S.J. Choi, Y.-H. Kim, Effect of amorphous silica and silica sand on removal of chromium(VI) by zero-valent iron, *Chemosphere*, 66 (2007) 858–865.
- [27] M. Moradi, R.R. Kalantary, T. Khosravi, H. Sharafi, K. Sharafi, Equilibrium isotherms and kinetic studies of lead removal from aqueous solution by pumice powder, *Technol. J. Eng. Appl. Sci.*, 5 (2015) 69–79.
- [28] M. Moradi, A.M. Mansouri, N. Azizi, J. Amini, K. Karimi, K. Sharafi, Adsorptive removal of phenol from aqueous solutions by copper (Cu)-modified scoria powder: process modeling and kinetic evaluation, *Desal. Wat. Treat.*, 57 (2016) 11820–11834.
- [29] N. Öztürk, T.E.L. Bektaş, Nitrate removal from aqueous solution by adsorption onto various materials, *J. Hazard. Mater.*, 112 (2004) 155–162.
- [30] M. Islam, R. Patel, Synthesis and physicochemical characterization of Zn/Al chloride layered double hydroxide and evaluation of its nitrate removal efficiency, *Desalination*, 256 (2010) 120–128.
- [31] Y.H. Liou, S.-L. Lo, C.-J. Lin, W.H. Kuan, S.C. Weng, Chemical reduction of an unbuffered nitrate solution using catalyzed and uncatalyzed nanoscale iron particles, *J. Hazard. Mater.*, 127 (2005) 102–110.
- [32] Q. Hu, N. Chen, C. Feng, W. Hu, Nitrate adsorption from aqueous solution using granular chitosan-Fe³⁺ complex, *Appl. Surf. Sci.*, 30 (2015) 1–9.
- [33] M. Moradi, L. Hemati, M. Pirsahab, K. Sharafi, Removal of hexavalent chromium from aqueous solution by powdered scoria-equilibrium isotherms and kinetic studies, *World Appl. Sci. J.*, 33 (2015) 393–400.
- [34] M. Jain, V.K. Garg, K. Kadirvelu, Adsorption of hexavalent chromium from aqueous medium onto carbonaceous adsorbents prepared from waste biomass, *J. Environ. Manage.*, 91 (2010) 949–957.
- [35] H. Wang, X. Yuan, Y. Wu, X. Chen, L. Leng, H. Wang, H. Li, G. Zeng, Facile synthesis of polypyrrole decorated reduced graphene oxide-Fe₃O₄ magnetic composites and its application for the Cr(VI) removal, *Chem. Eng. J.*, 262 (2015) 597–606.
- [36] J. Febrianto, A.N. Kosasih, J. Sunarso, Y.-H. Ju, N. Indraswati, S. Ismadji, Equilibrium and kinetic studies in adsorption of heavy metals using biosorbent: a summary of recent studies, *J. Hazard. Mater.*, 162 (2009) 616–645.
- [37] A. Mohseni-Bandpi, B. Kakavandi, R.R. Kalantary, A. Azari, A. Keramati, Development of a novel magnetite-chitosan composite for the removal of fluoride from drinking water: adsorption modeling and optimization, *RSC Adv.*, 5 (2015) 73279–73289.
- [38] V.K. Gupta, C. Jain, I. Ali, S. Chandra, S. Agarwal, Removal of lindane and malathion from wastewater using bagasse fly ash—a sugar industry waste, *Water Res.*, 36 (2002) 2483–2490.
- [39] R.R. Kalantary, A. Azari, A. Esrafil, K. Yaghmaeian, M. Moradi, K. Sharafi, The survey of Malathion removal using magnetic graphene oxide nanocomposite as a novel adsorbent: thermodynamics, isotherms, and kinetic study, *Desal. Wat. Treat.*, 57 (2016) 28460–28473.

Supplementary information

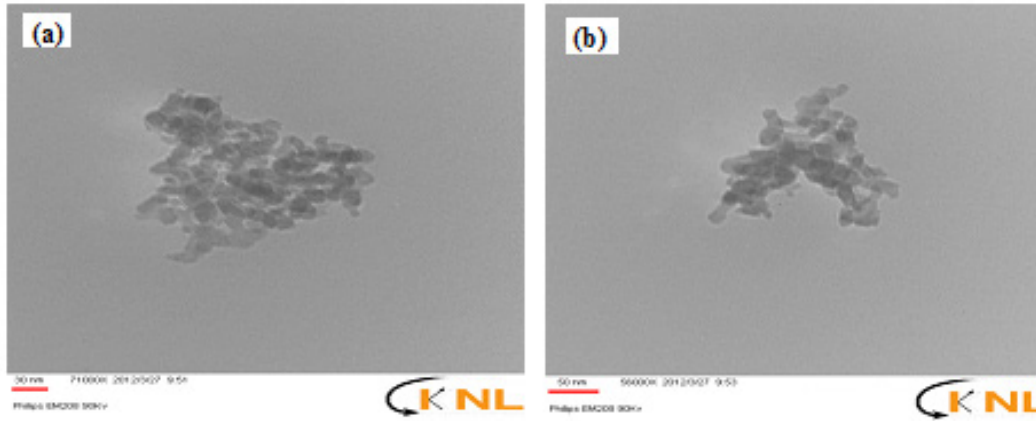


Fig. S1. TEM images of nZVI-zeolite samples 30 nm (a) and 50 nm (b).

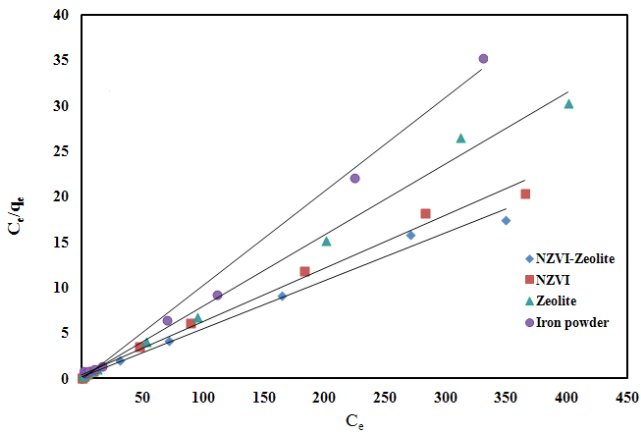


Fig. S2. The plots of Langmuir isotherm model for the adsorption of nitrate on different adsorbents.

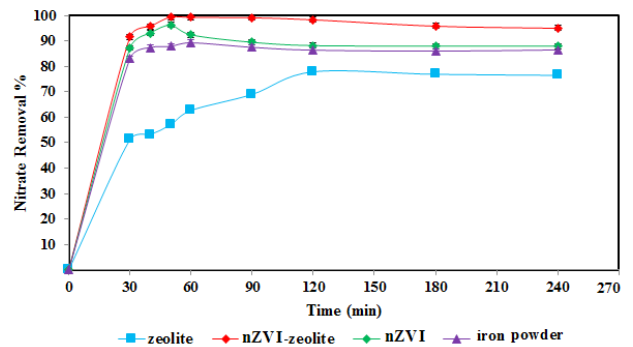


Fig. S4. The effect of contact time on nitrate adsorption by different adsorbents.

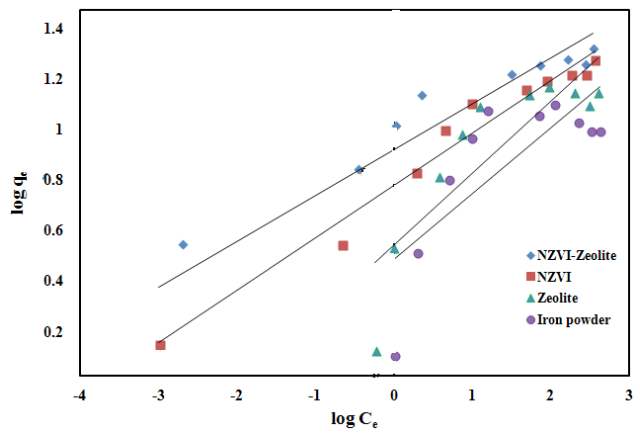


Fig. S3. The plots of Freundlich isotherm model for the adsorption of nitrate on different adsorbents.

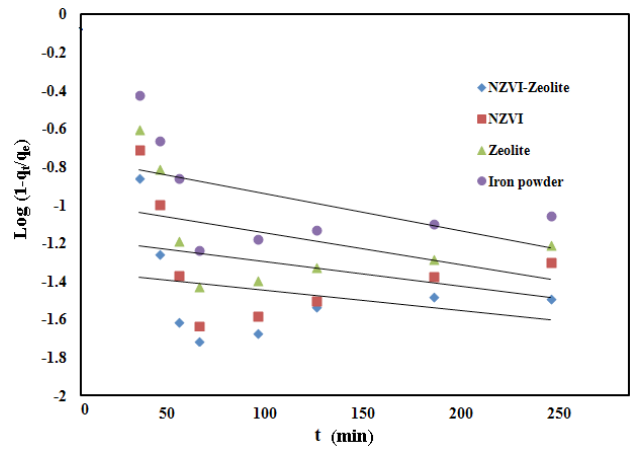


Fig. S5. The plots of pseudo-first-order model for the adsorption of nitrate on different adsorbents.

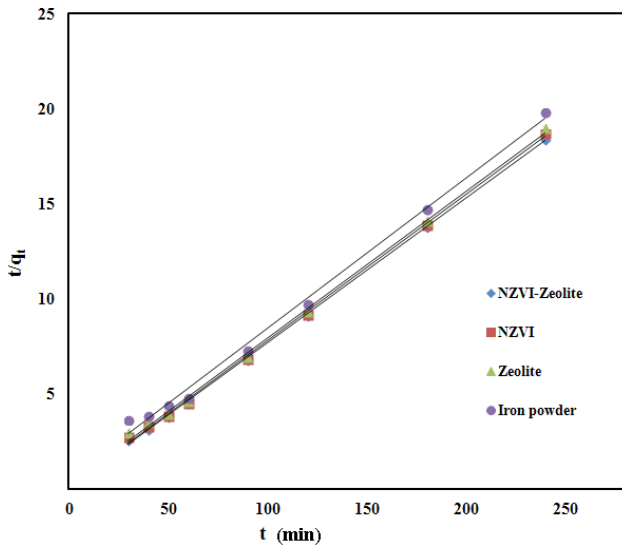


Fig. S6. The plots of pseudo-second-order model for the adsorption of nitrate on different adsorbents.

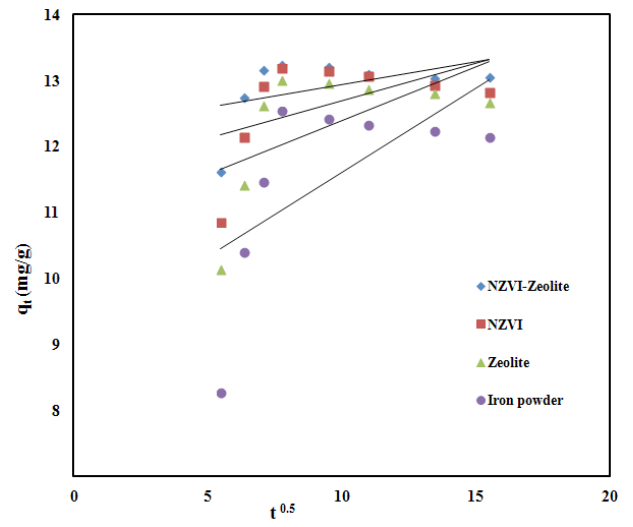


Fig. S7. The plots of intraparticle model for the adsorption of nitrate on different adsorbents.